



FDPS cooperates with PTEN loss to promote prostate cancer progression through modulation of small GTPases/AKT axis

Parthasarathy Seshacharyulu¹ · Satyanarayana Rachagani¹ · Sakthivel Muniyan¹ · Jawed A. Siddiqui¹ · Eric Cruz¹ · Sunandini Sharma¹ · Ramakrishnan Krishnan¹ · Brigham J. Killips¹ · Yuri Sheinin² · Subodh M. Lele² · Lynette M. Smith³ · Geoffrey A. Talmon² · Moorthy P. Ponnusamy^{1,4} · Kaustubh Datta^{1,4} · Surinder K. Batra^{1,2,4}

Received: 4 September 2018 / Revised: 15 January 2019 / Accepted: 3 March 2019 / Published online: 26 March 2019
© Springer Nature Limited 2019

Abstract

Farnesyl diphosphate synthase (FDPS), a mevalonate pathway enzyme, is highly expressed in several cancers, including prostate cancer (PCa). To date, the mechanistic, functional, and clinical significance of FDPS in cancer remains unexplored. We evaluated the FDPS expression and its cancer-associated phenotypes using in vitro and in vivo methods in PTEN-deficient and sufficient human and mouse PCa cells and tumors. Interestingly, FDPS overexpression synergizes with PTEN deficiency in PTEN conditionally knockout mice ($P < 0.05$) and expressed significantly higher in human ($P < 0.001$) PCa tissues, cell lines, and murine tumoroids compared to respective controls. In silico analysis revealed that FDPS is associated with increasing Gleason score, PTEN functionally deficient status, and poor survival of PCa. Ectopic overexpression of *FDPS* promotes oncogenic phenotypes such as colony formation ($P < 0.01$) and proliferation ($P < 0.01$) through activation of AKT and ERK signaling by prenylating Rho A, Rho G, and CDC42 small GTPases. Of interest, knockdown of FDPS in PCa cells exhibits decreased colony growth and proliferation ($P < 0.001$) by modulating AKT and ERK pathways. Further, genetic and pharmacological inhibition of PI3K but not AKT reduced FDPS expression. Pharmacological targeting of FDPS by zoledronic acid (ZOL), which is already in clinics, exhibit reduced growth and clonogenicity of human and murine PCa cells ($P < 0.01$) and 3D tumoroids ($P < 0.02$) by disrupting AKT and ERK signaling through direct interference of small GTPases protein prenylation. Thus, FDPS plays an oncogenic role in PTEN-deficient PCa through GTPase/AKT axis. Identifying mevalonate pathway proteins could serve as a therapeutic target in PTEN dysregulated tumors.

Introduction

Prostate cancer (PCa) is the second-most common malignancy affecting US men, with an estimated 174,650 new cases and 31,620 deaths in 2019 [1]. Treatment options for patients with localized PCa include active surveillance, surgery, external beam radiation therapy, and brachytherapy. Locally advanced and metastatic PCa patients are managed with a combination of radiotherapy (RT) with androgen deprivation therapy (ADT), whereas metastatic PCa patients are given ADT with chemotherapy/immunotherapy [2]. Though the initial response to ADT is appreciable, relapses occur after 2 years with the emergence of castration-resistant and highly aggressive disease, and life expectancy of 16–18 months [3]. The ineffectiveness of ADT is conferred by the accumulation of intratumoral androgens synthesized from the mevalonate pathway, important in cholesterol biosynthesis [4]. A recent study suggests that dysregulation of mevalonate pathway is

Supplementary information The online version of this article (<https://doi.org/10.1038/s41388-019-0791-9>) contains supplementary material, which is available to authorized users.

✉ Surinder K. Batra
sbatra@unmc.edu

¹ Department of Biochemistry and Molecular Biology, University of Nebraska Medical Center, Omaha, NE, USA

² Department of Pathology and Microbiology, University of Nebraska Medical Center, Omaha, NE, USA

³ Department of Biostatistics, University of Nebraska Medical Center, Omaha, NE, USA

⁴ Fred and Pamela Buffett Cancer Center, Eppley Institute for Research in Cancer and Allied Diseases, University of Nebraska Medical Center, Omaha, NE, USA

associated with PTEN loss and emergence of castration-resistant and androgen-independent PCa [5]. Furthermore, several epidemiological reports suggest that a moderate increase (10 mg/dL) in serum cholesterol was associated with 9% risk of PCa recurrence [6]. The significance of tumor suppressor PTEN loss was found to be associated in 38% of primary PCa patients and 50% of metastatic PCa [7]. Earlier studies in PCa mouse models demonstrated the implications of PTEN loss and its association with the pre-neoplastic stages (hyperplasia and prostatic intraepithelial neoplasia {PIN}) followed by tumorigenesis and metastasis, specifically, lymph node, and lung metastasis [8]. In support of these findings, the most recent deep sequencing analysis identified that PTEN is inactivated in 50% of PCa predominantly due to copy number alterations [9–11]. Therefore, we need to understand the mechanism by which the mevalonate pathway is deregulated as a consequence of PTEN inactivation in PCa and to re-purpose FDA-approved drugs targeting cholesterol biosynthesis.

Our previous study demonstrated that a differential expression pattern of the majority of genes involved in the mevalonate pathway (FDPS, ACAT2, DHCR7, SC4MOL, and SQLE) was associated with radioresistance in pancreatic cancer [12]. Among the mevalonate pathway genes, FDPS (farnesyl diphosphate synthase) was found to be associated with PCa aggressiveness and biochemical recurrence [13]. In addition, a recent global RNA sequencing analysis of PCa tissues revealed FDPS as one of the top differentially expressed genes associated with PCa progression, advancement, and biochemical recurrence [14]. FDPS is a pleiotropic enzyme that catalyzes production of geranyl diphosphate and farnesyl diphosphate (FDP) from isopentenyl pyrophosphate and dimethyl-allyl pyrophosphate. FDPS plays a critical role in cholesterol biosynthesis (CBS) and protein prenylation [15]. During the post-translational modification process, farnesyl transferase (FTase) catalyzes the transfer of farnesyl group from FDP to small GTPases such as Ras, Rho, Rac, Rab, and Rap1a proteins, enabling them for membrane anchorage and cellular signaling [16]. Mevalonate pathway enzymes (including FDPS) were investigated over several decades for their physiological function, but their dysregulated role in several cancers including PCa was largely unknown.

Earlier studies showed that ZOL, the third generation of nitrogen-containing bisphosphonates, was effective in inhibiting the proliferation, survival, and bone metastasis of PCa cells [17]. NMR and crystallography studies have further revealed that FDPS is a key target of nitrogen-containing bisphosphonates (N-BPs) [18]. Several pre-clinical and clinical studies have demonstrated the additive and synergistic effects of ZOL when combined with various cytotoxic agents in various cancers [19–22]. However, its inhibitory action on key enzymes in the mevalonate

pathway and their associated mechanism(s) in cancer therapy is poorly understood.

In the present study, we analyzed the expressional variation of FDPS in a spectrum of human PCa tissues and normal counterparts. FDPS was differentially expressed in the PTEN-deficient cells as compared to PTEN-sufficient PCa cells. Our PTEN conditional knockout (cKO) murine model revealed that FDPS is specifically upregulated upon loss of the PTEN tumor suppressor together with activation of the PI3K/AKT pathway. Further, the oncogenic role of FDPS and its associated mechanism were defined using 2D and 3D models in PTEN-sufficient and -deficient PCa cells. Finally, our study validated whether FDPS should be targeted in PTEN-functionally deficient PCa cells or PTEN wild-type (PTEN^{WT}) PCa cells.

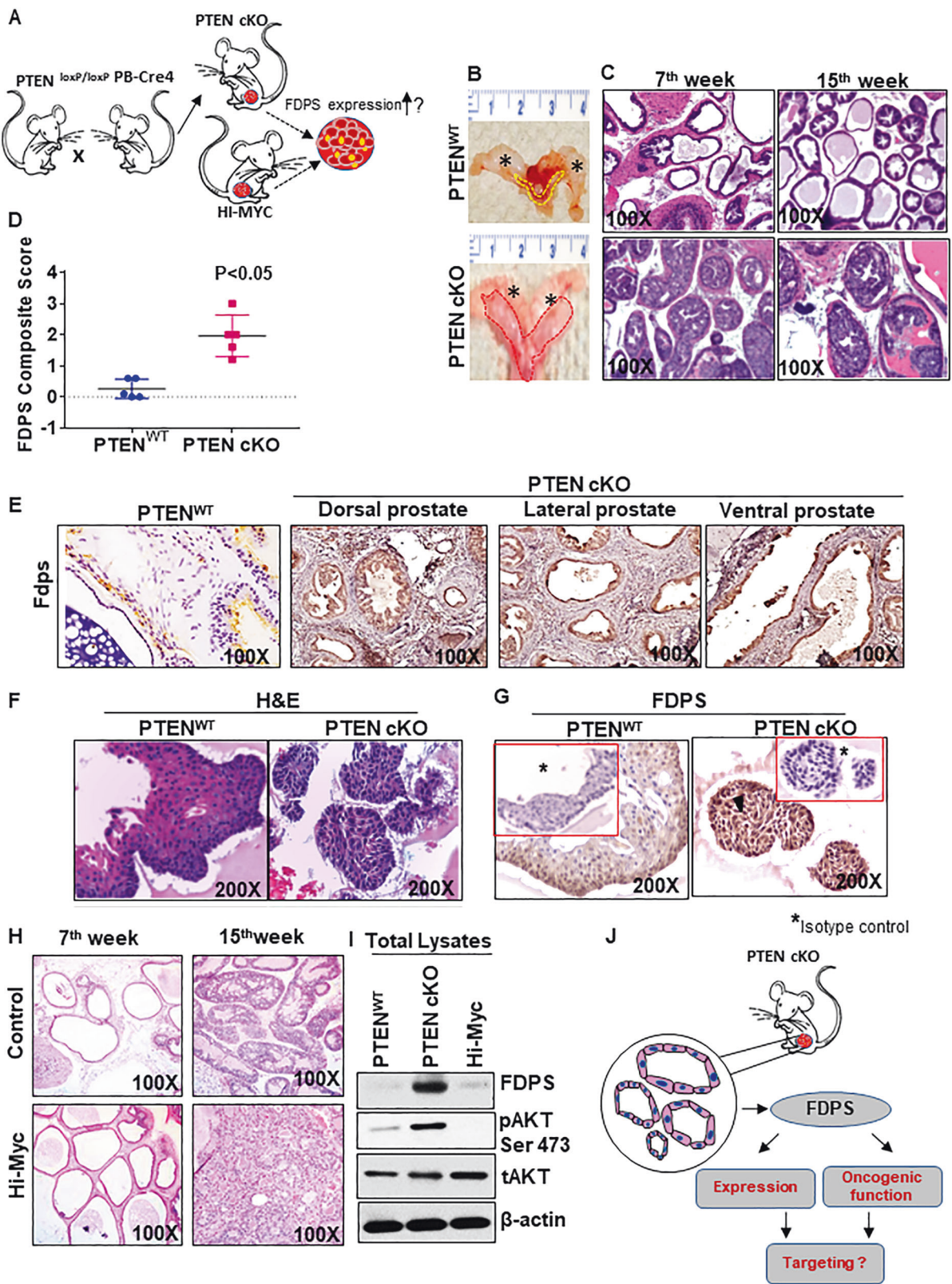
Results

FDPS is specifically elevated in the PTEN conditional knockout autochthonous tumors

To examine the deregulation of FDPS in PCa, PTEN cKO mouse model (PTEN^{loxP/loxP}; Pb-Cre4⁺) tumor and its derived tumoroids were utilized (Fig. 1a, Supplementary Fig. S1A). Histopathological variation in the prostate tissue of 7- and 15-week PTEN cKO mice was observed with the low- and high-grade PINs and adenocarcinoma, compared with littermate control mice (Fig. 1b, c, Supplementary Fig. S1B), as described previously [23]. The PTEN cKO mice exhibited significantly higher FDPS staining intensity compared to littermate controls ($P < 0.05$) (Fig. 1d). Immunoreactivity of FDPS was greater in all prostatic lobes of PTEN cKO mice, but a basal-to-low expression of FDPS was observed in the control mice (Fig. 1e, Supplementary Fig. S1C). Similarly, FDPS expression was increased in histology matched tumoroids compared to control organoids (Fig. 1f, g). The expression of FDPS in an in vivo mouse progression and 3D models suggests that FDPS activation and expression are associated with the oncogenic transformation of PCa.

FDPS is specifically modulated in PTEN cKO mice but not in Hi-Myc mice

To examine whether the increased FDPS expression in PTEN cKO mice is due to lack of PTEN activity alone and not due to any other oncogene, which is similar in elucidating pathophysiological function or activity of another oncogene, we acquired Hi-Myc transgenic animals. Initially, we observed the similarities such as (Prostatic intraepithelial neoplasia) PIN lesions and PCa histotypes of Hi-Myc and PTEN cKO at 7 and 15 weeks of age (Fig. 1h),



as described previously [24]. Whole prostate tissue lysates from PTEN^{WT}, PTEN cKO, and Hi-Myc (Supplementary Fig. S1D (genotype validation)) mice were immunoblotted

with FDPS, activated AKT (pAKT Ser 473), and actin antibodies. As shown in Fig. 1i, PTEN cKO expressed higher levels of FDPS and pAKT compared with Hi-Myc

◀ **Fig. 1** FDPS expression in prostate tissues and 3D organoid culture derived from normal and prostate cancer tissues of PTEN cKO mouse model. **a** Development of mouse models of prostate cancer to detect FDPS levels. PTEN cKO mouse model-derived prostate tissues, organoids, and tumoroids were subjected to immunohistochemical analysis by staining with antibody specific for FDPS as indicated in material and methods. **b** Murine urogenital organs such as bladder, seminal vesicle, and prostate were excised from 15-week-old PTEN cKO and PTEN^{WT} control mice and examined for gross morphology. The asterisk represents the seminal vesicle. Dotted lines show normal and enlarged prostate excised from the wild-type (yellow) and PTEN cKO (red) mice. **c** Histological analysis of mouse prostate cancer model. Representative images showing hematoxylin and eosin staining in mouse prostate dorsolateral lobes of PTEN^{WT} and PTEN cKO mice at 7 and 15 weeks of age. **d** Box plot shows an increase in mean composite score of FDPS expression in mouse prostate of PTEN cKO mice compared with age-matched prostate tissues of PTEN^{WT} animal. **e** Immunohistochemical detection of FDPS protein in various lobes of mouse tissues. FDPS is highly expressed in epithelial cells of PTEN cKO prostate cancer tissues compared to PTEN^{WT}. **f, g** Representative image of a normal prostate organoid stained with hematoxylin and eosin (left) and FDPS antibody (right). **g** Positive immunoreactivity is shown for FDPS. Serial sections of the same tumoroids and organoids used for FDPS staining were evaluated with non-specific isotype control antibodies (Insert). **h** Representative histological sections with hematoxylin and eosin staining of prostate tissues of wild type (top) and Hi-Myc-driven transgenic mouse (bottom) at 7 and 15 weeks of age. **i** Western blot analysis of FDPS, pAKT, and total AKT expression in the total lysates isolated from prostates of 15-week-old WT, PTEN cKO, and Hi-Myc-driven mice. **j** Schematic diagram showing the application of tumoroids isolated from the prostate-specific PTEN cKO mouse model to be used for FDPS expression analysis

and PTEN^{WT} control mice. These data suggest that deletion of PTEN and subsequent activation of PI3K/AKT pathway in part induces FDPS expression for its oncogenic function in PCa (Fig. 1j).

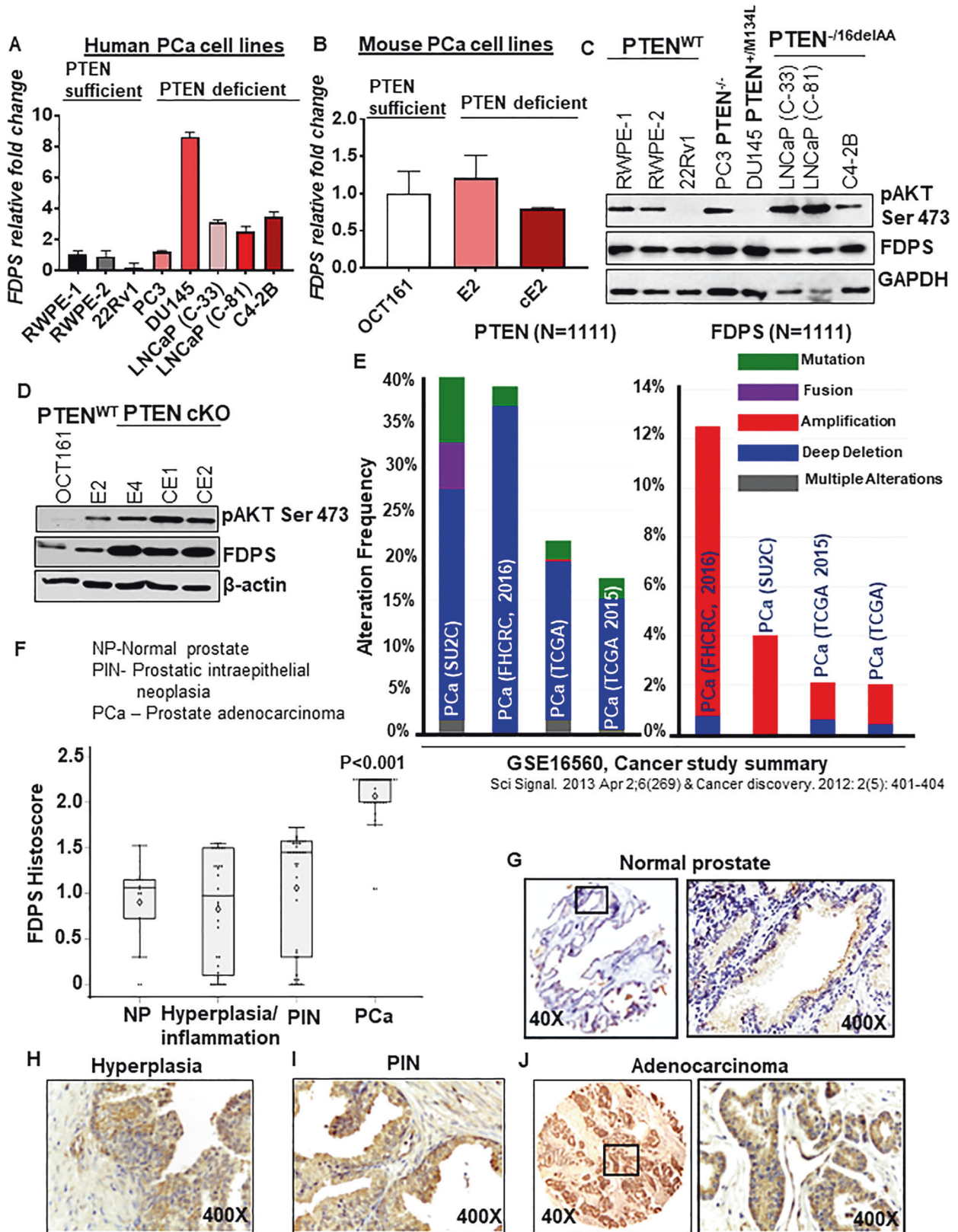
FDPS is overexpressed specifically in PTEN-deficient human and mouse PCa cell lines

To characterize the expression pattern of FDPS in PCa cells, a panel of human and mouse PCa cell lines were analyzed for FDPS expression at the mRNA and protein levels (Fig. 2a, b). PCa cell lines had a 0.18- to 8.6-fold increase in FDPS mRNA expression compared to the normal immortalized RWPE-1 and -2 cell lines (Fig. 2a). FDPS protein levels were also elevated in the majority of PTEN-deleted/mutated PCa cells lines relative to RWPE-1, -2 and 22Rv1 PTEN^{WT} cells. FDPS expression at protein and RNA levels strongly correlated with the activated form of AKT in human and mouse PCa cell lines (Fig. 2c, d). Mouse syngenic cell line is an excellent tool to determine whether specific PTEN cKO has an impact on desired genes and their respective protein products. For this purpose, we developed and characterized (genotyping) normal prostate epithelial cell lines from PTEN^{WT} harboring mouse (negative for Pb-Cre expression) and labeled as OCT 161 (Supplementary Fig. S2A). As shown in Fig. 2b, d, FDPS relative mRNA and protein

expression levels are higher in PTEN cKO mouse-derived syngenic cell lines (E2, E4, cE1, and cE2) as compared to normal prostate epithelial syngenic cell line (OCT161). Similarly, we also observed an increase in AKT phosphorylation (Fig. 2d) along with a series of small GTPase Rho A, Rho G, and CDC42 in PTEN cKO mouse-derived syngenic cell lines (E2, E4, cE1, and cE2) as compared to normal prostate epithelial syngenic cells (Supplementary Fig. S2B). To confirm the relative growth rate between FDPS high expressing mouse PCa cells and FDPS basal expressing normal-derived cells, we performed colony formation assay. We observed that FDPS overexpressing E2, cE1, and cE2 PTEN cKO cell lines exhibited significantly large number of colonies, large in size and grew faster than PTEN^{WT}-derived normal cells (OCT161) (Supplementary Fig. S2c, d). In addition, morphological analysis of OCT 161 and E2 (FDPS low and basal cell lines) displayed dispersed cell distribution pattern with loss of cell to cell contact whereas, FDPS, pAKT, and small GTPases high expressing cE1 and cE2 cells showed larger colony growth (clumpy) with a high cell to cell contact (Supplementary Fig. S2e). *FDPS* was amplified and its frequency coincided with PTEN deletion/mutation (cBioPortal platform) (24) (Fig. 2e). Specifically, the tendency of *FDPS* amplification is significantly ($P = 0.016$) associated with PTEN deletion status in the cBioportal database (Prostate Adenocarcinoma, Fred Hutchinson CRC cohort). These data indicate that loss of PTEN coupled with post-transcriptional and translational modulation of FDPS may lead to aggressive nature of PCa.

Expression of FDPS protein in pre-neoplastic and neoplastic prostate tissues

The intensity of FDPS staining in the spectrum of prostate tissues (Normal, hyperplasia, PIN, and PCa) was scored, and a statistically significant difference in FDPS expression was observed between PCa tissues vs. normal prostate ($P < 0.001$), and between PIN vs. PCa ($P < 0.001$) (Fig. 2f). In a total of 14 normal/normal adjacent to tumor (NAT) tissues, FDPS protein expression was negative in 2 (14.28%), low/basal in 11 (78.57%), and weak in 1 (7.14%) (Fig. 2g). FDPS staining intensity in hyperplasia and inflammatory tissues scored between 1.5 and 1.75 (weak) and <1.5 (low/basal) (Fig. 2h). FDPS staining was prominent in the prostate epithelial cells of PIN and PCa lesions, but negative in the stromal region (Fig. 2i, j). In addition, the two tissue cores representing the lymph node and coastal bone metastasis tissues stained strongly for FDPS (Supplementary Fig. S3A). In addition, FDPS was overexpressed in metastatic PCa as compared to primary PCa tissues (Supplementary Fig. S3B). Our data suggest that FDPS expression could correspond with the disease state, increasing from normal to the pre-neoplastic condition and peaking during PCa progression and advancement.



◀ **Fig. 2** FDPS is differentially regulated in prostate adenocarcinoma and PTEN-deficient human and murine prostate cancer cells as compared to respective normal tissues/PTEN^{WT} counterparts. **a–d** FDPS mRNA and protein expression was screened in a panel of human and mouse prostate cancer cell lines differing by PTEN mutation/deletion status. Total RNA was isolated from indicated human and mouse normal and prostate cancer cell lines and subjected to semi-quantitative RT-PCR. **a** Relative fold change of *FDPS* expression in a normal immortalized prostate epithelial cell line and a panel of prostate cancer cell lines was normalized with the Ct value of GAPDH. The bar represents the average of triplicate samples. **b** FDPS relative mRNA expression was analyzed by semi-quantitative RT-PCR in normal prostate-derived and PTEN cKO mouse-derived syngeneic cell lines. **c, d** Western blot analysis of FDPS and phosphorylated AKT expression in a panel of human and mouse prostate cancer cell lines. **e** Bar graph showing concordance of *FDPS* gene amplification and *PTEN* deletion/mutation status in same PCa cohorts using CBioportal. **f** Box plot shows a significant increase in the mean FDPS intensity in prostate adenocarcinoma tissues and PIN lesions compared to hyperplasia and normal prostate tissues ($P < 0.001$). **g–j** Images represent FDPS immunohistochemical staining in prostate tissues, **g** normal prostate, **h** hyperplasia, **i** PIN, and **j** prostate adenocarcinoma

Table 1a Number of pathological tissue types and percentage

Tissue type	<i>N</i>	%
Malignant	35	28.46
PIN	42	34.15
Hyperplasia/Inflammation	32	26.02
Normal/NAT	14	11.38

FDPS expression and its association with clinicopathological characteristics

The pathological tissue types and combination groups are shown in Table 1a, b. The Kruskal–Wallis test showed significant differences in composite score between groups (Supplementary Table S1, Fig. 2f). Pairwise comparisons in Supplementary Table S1 showed that the PCa group has significantly higher composite scores than other groups. FDPS expression was decreased in an order from malignant, PIN, hyperplasia/inflammation, and normal/NAT (Fig. 2f). Next, composite scores were correlated with clinicopathological characteristics in the PCa (malignant) group (excluding small acinous carcinoma). Composite scores did not differ by stage ($P = 0.53$) or by Gleason score categorized at the median ($P = 0.22$). However, we observed significantly higher composite scores in grades 3–4 PCa tissues ($P = 0.0004$) (Supplementary Tables S2 and S3). In addition, our database analysis of PCa tissues showed a strong association of FDPS expression between two Gleason score (GS) pattern (GS 5–6 vs GS9, $P < 0.01$) (Supplementary Fig. S3C). The normal/NAT group was significantly younger than the other three groups, which were not significantly different from each other in age (Supplementary Table S4).

Ectopic expression of FDPS in PTEN functionally inactivated PCa cells elicit an aggressive phenotype

To investigate the functional role and potential mechanism (s) of FDPS in PTEN-deficient and -sufficient PCa cells (Fig. 3a), the full-length FDPS gene (Supplementary Fig. S4A, S4B) was ectopically overexpressed in 22Rv1 and C4-2B PCa cells. Western blot and confocal analysis showed detection of FDPS in 22Rv1 and C4-2B PCa cells (Fig. 3b, c). Next, colony formation and growth kinetics assays were performed to characterize the functional significance of FDPS in PCa cells. A significantly increased number of colonies was observed in FDPS-overexpressed PTEN^{-/-} (PTEN deficient) PCa cells as compared to PTEN-sufficient PCa ($P < 0.01$) (Fig. 3d). Similarly, enhanced proliferation was observed when FDPS was overexpressed in Pten-deficient PCa cells ($P < 0.01$) compared to wild-type 22Rv1 cells (Fig. 3e). These results confirm that the enhanced cell growth and proliferation might be due to the introduction of FDPS in PTEN-deficient cells.

FDPS overexpression leads to activation of oncogenic signaling and changes in the prenylation of small GTPases

Since FDPS overexpression is associated with aggressiveness in PCa cells, we assessed the phosphorylation status of the most common oncogenic signaling molecules such as AKT, ERK, and STAT pathways. Ectopic overexpression of FDPS in PCa cells led to increased phosphorylation of AKT and ERK, with no change in their total protein levels along with increased cyclin B1 expression compared to vector-transduced PCa cells (Fig. 4a). We subsequently analyzed whether the exogenous introduction of FDPS had an effect on proteins that mediate tumor suppressive pathways. Of note, loss of STAT1 was shown to promote tumor recurrence in PCa patients [25] and altered expression of FDPS was associated with tumor recurrence in PCa patients [13]. We found that FDPS overexpression significantly reduced phosphorylation of JAK1 and STAT1 at Ser727 and Tyr701, but did not affect total JAK1 and STAT1 proteins (Fig. 4a, Supplementary Fig. S4C). Our results suggest that FDPS overexpression in cancer cells could promote cancer progression by activating AKT and ERK signaling, or by disrupting the constitutively active JAK–STAT tumor suppressive signals in PCa, consistent with previous publication [26].

Using immunoblot analysis, the prenylation of Rho A, Rho G, and CDC42 was induced in FDPS ectopically overexpressed PCa cells compared to vector-transfected PCa cells (Fig. 4a). Overall, FDPS positively correlated with signaling molecules in both the PCa cells. These data point out the evolution of FDPS in the Pten-deficient PCa

Table 1b Relative comparison between groups and statistical significance

<i>p</i> -Value	Malignant vs PIN	Malignant vs Hyperplasia/ Inflammation	Malignant vs NAT/Normal	PIN vs Hyperplasia/ Inflammation	PIN vs NAT/ Normal	Hyperplasia/ Inflammation vs NAT/Normal
Unadjusted	<0.0001	<0.0001	<0.0001	0.0208	0.043	0.90
Adjusted*	<0.0001	<0.0001	<0.0001	0.12	0.26	1.0

**P* values adjusted for multiple comparisons with the Bonferroni method

Fig. 3 Ectopic overexpression of FDPS in PTEN-deficient PCa cells increases proliferation and growth advantage. **a** Schematic representation of predicted FDPS-mediated mechanism(s) in PCa cells. **b**, **c** p3Xflag-CMV-10-FDPS construct and empty vector were stably transduced with similar units in PTEN-sufficient 22Rv1 and PTEN-deficient C4-2B PCa cells. Subsequently, stably transfected cells were cultured with selection medium containing G418 at 300 µg/ml and clones were selected and analyzed for FDPS positivity using **b** western blot and **c** confocal analysis. **d** Box plot shows an increase in the average number of colonies in C4-2B PCa cells stably transfected with FDPS cDNA as compared to 22Rv1 cells. **e** Cells with FDPS overexpression or vector transduction were assessed for proliferative kinetics by a growth kinetics assay. Cells were measured for 7 days using a cellometer auto 1000 cell counter. The average number of FDPS-overexpressed cells was significantly higher compared to vector-transduced PCa cells

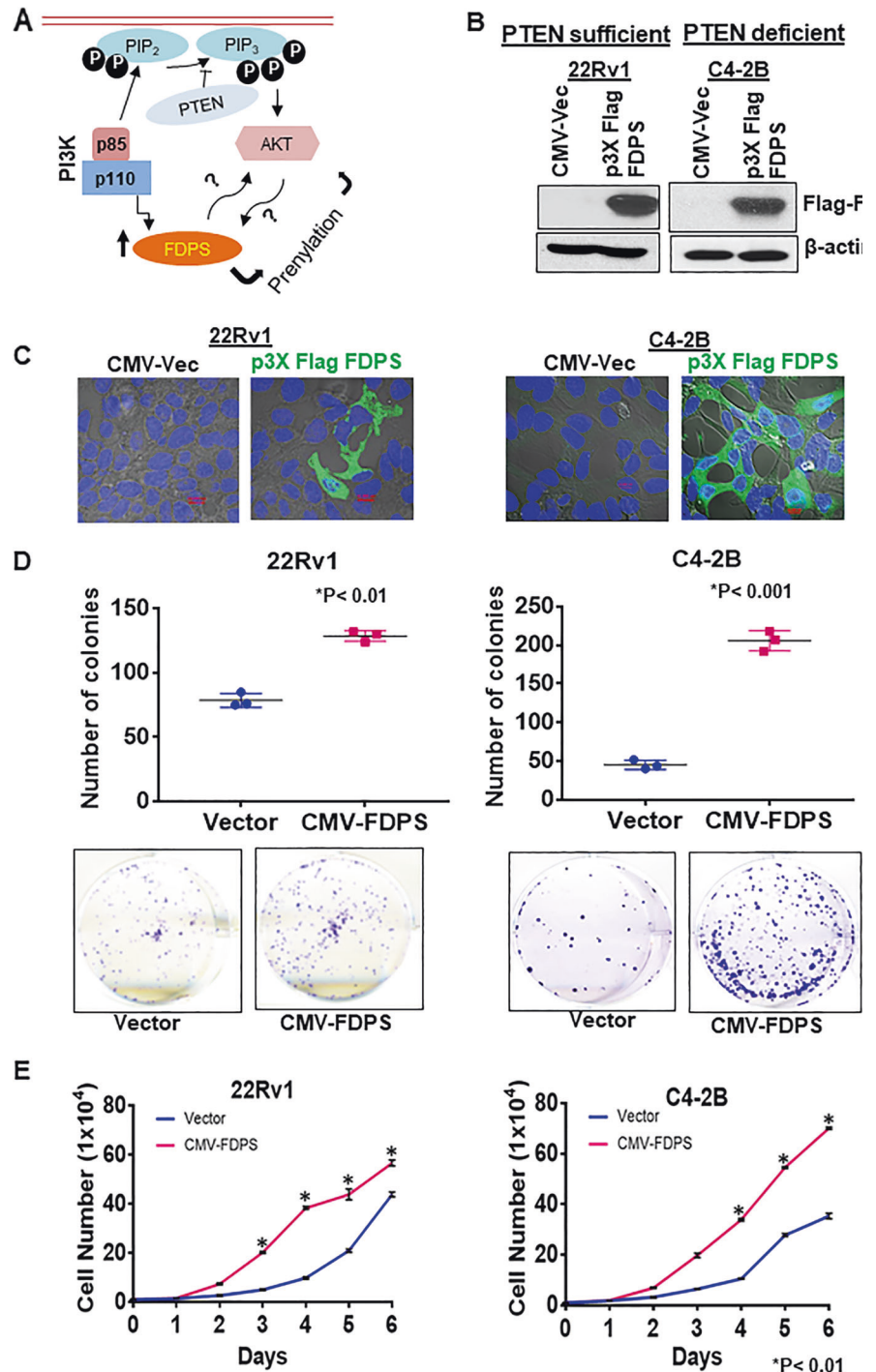
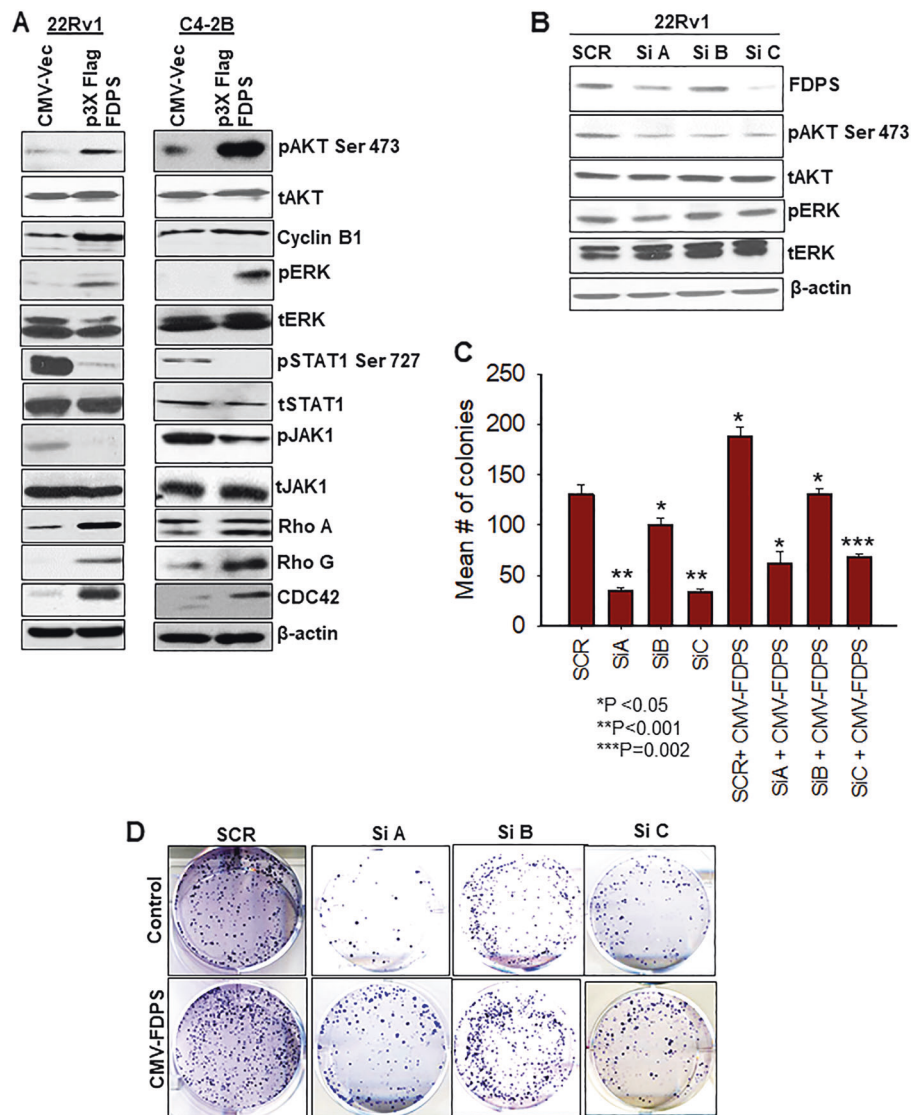


Fig. 4 FDPS-mediated oncogenic signaling was more pronounced in PTEN-deficient prostate cancer cells than PTEN^{WT} cells. **a** The p3x-FLAG-CMV-10-FDPS and CMV-10 vector-transduced cells were seeded at a density of 1×10^6 in a 60 mm dish and analyzed for signaling molecules (AKT, ERK, JAK1/STAT1, and FDPS) with respective phospho forms by western blot. β -actin served as an internal loading control. Immunoblot analysis detected the unphosphorylated and phosphorylated forms of RhoA, Rho G, and CDC42 proteins. Top band is the unphosphorylated form and bottom band represents the phosphorylated proteins. **b** PCa cells were transiently transfected with three siRNAs targeting FDPS. After 48 h transfection, cell lysates were harvested and analyzed using western blot for expression of FDPS, phospho AKT, and ERK with respective total forms. **c** Effect of gene silencing of FDPS on clonogenicity was tested in 22Rv1 PCa cells. Bars represent the average number of colonies in siRNA-transfected cells, relative to scramble siRNA-transduced cells ($N = 3/\text{group}$). **d** Representative images depict the reduction in the number of colonies upon FDPS knockdown



cells and explains the potential mechanism(s) underlying FDPS-mediated protein prenylation and its critical role in enhancing PCa cell aggravation.

FDPS knockdown affects AKT and ERK signaling and thereby impairs the colony-forming ability of PCa cells

Silencing of FDPS reduced p-AKT and pERK levels along with prenylation patterns of Rho A, G, and CDC42 small GTPases compared to control PCa cells (Figs. 4b and 5h). Furthermore, knockdown of FDPS significantly decreased the number of colonies ($P < 0.001$) compared to control cells. In addition, relative increased colony numbers were observed in FDPS KD PCa cells and scramble siRNA-transfected controls cells (bottom panel) when rescued using ectopic overexpression system (relative to respective controls (top panel)). However, the relative number of

colonies was less from cells transfected with FDPS-specific siRNA compared to PCa cells with scramble siRNA (Fig. 4c, d), suggesting that FDPS suppression could inhibit colony formation of PCa cells.

PI3 kinase pathway inhibition affects FDPS not the AKT pathway

To determine the effect of inhibiting PI3K/AKT pathway and its impact on FDPS, PCa cells were treated with pharmacological inhibitors and siRNA specific for selected genes. Initially, dose-dependent treatment with multi-targeted PI3K inhibitor (PI-103) in PTEN-sufficient 22Rv1 and PTEN-deficient C4-2B PCa cells for 24 h resulted in the decrease in PI3K isoforms p110 δ and p85 as compared to untreated control PCa cells (Fig. 5a). Increasing concentrations of PI-103 also resulted in the reduction of FDPS protein together with reduced phosphorylation of AKT and

ERK in C4-2B cells, while PI-103 treatment in 22Rv1 did not reduce FDPS (Fig. 5a, Supplementary Fig. S5A). However, a higher dose of PI-103 significantly decreased AKT and ERK phosphorylation in 22Rv1 cells (Fig. 5a). Further, to validate the specificity of PI3K inhibition and its impact on FDPS, we performed transient (72 h) silencing of *PI3K* in another PTEN-deficient LNCaP (C-81) PCa cell line. We observed that FDPS protein expression was reduced upon silencing of *PI3K* as compared to scramble siRNA-transfected PCa cells (Fig. 5b). To observe the influence of AKT on FDPS, which is downstream of PI3K, we treated both the PTEN-sufficient and -deficient PCa cells with AKT-specific inhibitor MK-2206 or siRNA. MK-2206 dose-dependently inhibited AKT phosphorylation without affecting FDPS protein levels in C4-2B cells while AKT inhibitor affected AKT phosphorylation only at the higher dose in 22Rv1 cells (Fig. 5c). Further, we performed AKT specific siRNA mediated gene knockdown studies (48 h) in two PTEN-deficient PCa cells (C4-2B and LNCaP (C-81) to observe its impact on FDPS expression (Fig. 5d). We found that pharmacological or siRNA treatment against AKT did not affect FDPS protein expression. Taken together, our data suggest PI3K, rather than direct AKT pathways, mediates FDPS regulation.

In addition to PI3K signaling, we also observed that AR signaling activation by 5 α -dihydrotestosterone (DHT) treatment increases FDPS level. We performed the DHT treatment on androgen-sensitive LNCaP (C-33) cells as a time course experiment. LNCaP (C-33) cells were initially serum starved and treated with DHT at 10 nM concentration for 48 h. As shown in Supplementary Fig. S5B, the protein expression of FDPS was elevated by 8–10-folds upon DHT treatment. To assess the most common gene responsive for AR activation, we checked the expression of cellular PSA, culture supernatant PSA level in the same lysate analyzed for FDPS protein expression. We observed a complete activation of PSA in the DHT treatment LNCaP cells compared to the DHT untreated parental cells. Further, to confirm the influence of p53 (a well-established player in PCa) upon FDPS expression, we performed transient silencing of p53 in PTEN-deficient PCa cell lines. We observed that FDPS protein expression was affected upon silencing p53 (72 h) (Supplementary Fig. S5C). These results suggest that AR signaling regulating FDPS could be a major factor responsible for the synthesis of intratumoral androgen within the PCa cells.

Pharmacological inhibition of FDPS using ZOL inhibits AKT and ERK pathways

We examined the growth inhibitory effect of ZOL in time- and dose-dependent manner on various human and mouse PCa cell lines using MTT assay. Treatment of PCa cells

with ZOL concentration ranging from 7.5 to 22.5 μ M concentrations exhibited mixed efficacy and depending on the cell type. Majority of human and mouse PCa cell lines showed IC₂₅ and IC₅₀ values of 7.5 and 17.5 μ M concentrations (Supplementary Fig. S6). To test whether the growth inhibitory effect of ZOL was due to direct negative modulation of FDPS protein, we treated PCa cells with ZOL (ranging from 0 to 20 μ M concentrations) for 24 h. As shown in Fig. 5e, ZOL dose-dependently decreased FDPS protein expression at all the tested concentrations in both PTEN-deficient LNCaP C-81 and C4-2B PCa cells, whereas PTEN-sufficient 22Rv1 cells showed moderate FDPS modulation only at 20 μ M concentration. These results suggest that the reduction in cell viability upon ZOL treatment in PTEN-deficient PCa cells correlates with FDPS targeting by ZOL. Further, to examine the effect of ZOL on FDPS downstream targets AKT and ERK, we treated PTEN-deficient and -sufficient PCa cells with 20 μ M concentration of ZOL and performed western blot analysis. Our data show that phosphorylation of AKT and ERK were affected by ZOL along with FDPS protein reduction (Fig. 5f). In addition, to determine whether statins targeting HMG-CoA reductase affects FDPS protein expression, we treated the PTEN-sufficient and -deficient PCa cells with two different kind of statins (simvastatin and fluvastatin). Dose-dependent treatment with simvastatin and fluvastatin on 22Rv1 cells had no impact on FDPS expression. In contrast, a marginal increase in FDPS expression was observed in PTEN-deficient C4-2B cells (Supplementary Fig. S7). These results imply that a marginal increase in FDPS levels could be associated with compensatory mechanism arise as a result of HMG-CoA enzyme inhibition which is upstream of FDPS.

Next, we analyzed whether ZOL inhibition of FDPS prevents prenylation of small GTPases in PCa cells. PCa cells were exposed to various doses (0–20 μ M) of ZOL for 24 h, and protein lysates were analyzed for the prenylated and unprenylated forms of Rho A, Rho G, CDC42, and Ras proteins. As shown in Fig. 5g, ZOL dose-dependently increased unprenylated forms while decreasing the prenylated Rho A, Rho G, and CDC42 small GTPases in C4-2B cells. Whereas, ZOL has little effect on small GTPases prenylation in 22Rv1 cells. H-Ras prenylation was not altered in 22Rv1 cells at all doses of ZOL, whereas 20 μ M ZOL moderately increased H-ras prenylation in C4-2B cells. Thus, decreases in phosphorylation of AKT and ERK is confirmed by parallel inhibition of small GTPases in PCa cells. These results were further validated using siRNA specific for FDPS in PCa cells and cell lysates were analyzed for Rho A, Rho G, and CDC42 small GTPases. As expected, FDPS knockdown increased the ratio of unprenylated vs prenylated forms of small GTPases (Fig. 5h).

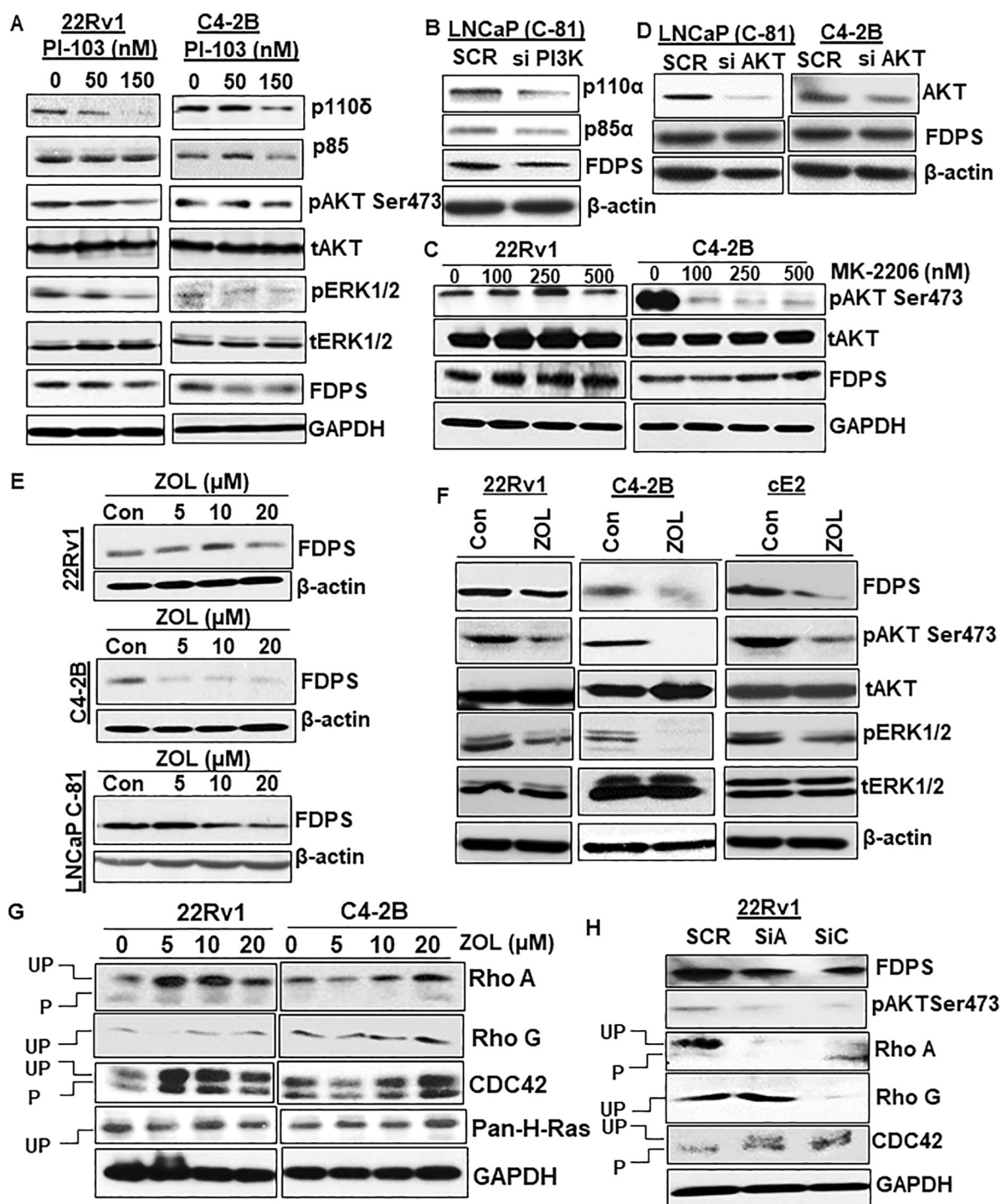


Fig. 5 Pharmacological and genetic inhibition of PI3K or FDPS affects small GTPases/AKT axis. **a, b** PTEN-deficient C4-2B and PTEN-sufficient 22Rv1 cells were treated with and without PI3K-specific PI-103 or PI3K-specific siRNA for 24 and 72 h, respectively. Total lysates were immunoblotted and probed with PI3K subunits anti-p110 α , anti-p110 δ and anti-p85, anti-phospho AKT, anti-phospho ERK and anti-FDPS antibodies. **c, d** Effect of AKT-specific MK-2206 inhibitor or siRNA alone treatment in PCA cells. **e** Dose-dependent effect of ZOL on 22Rv1, C4-2B, and LNCaP C-81 PCA cells. After 48 h exposure to ZOL, cells were lysed and subjected to western blot to detect FDPS protein expression. ZOL induces a dose-dependent decrease in FDPS protein, specifically at 20 and 40 μ M concentration in PCA cells. **f** Effect of ZOL on inhibition of FDPS levels with ERK and AKT phosphorylation determined using western blot in 22Rv1, C4-2B, and cE2 sublines. **g** PCA cells were cultured in the presence of indicated doses of ZOL, and total protein lysates were analyzed for ZOL-mediated inhibition of prenylation of RhoA, Rho G, CDC42, and H-Ras proteins. **h** FDPS siRNA- and scramble siRNA-transfected PCA cells were analyzed for suppression of protein prenylation using indicated antibodies

In addition, we further performed immunofluorescence analysis using anti-Rho A and anti-Rho G antibodies in PCa cells to verify whether inhibition of prenylation by ZOL affects the subcellular distribution of small GTPases. PTEN-deficient C4-2B PCa cells treated with ZOL (20 μ M) showed higher cytosolic accumulation of Rho A and Rho G, while PTEN-sufficient 22Rv1 cells showed only Rho A in the cytoplasmic compartment but not Rho G. Untreated control PCa cells exhibited majorly membranous localization of Rho A and Rho G (Supplementary Fig. S8). Further, we evaluated the similarity in the mode of action of ZOL and farnesyl transferase inhibitors (Ftases) I and II in inhibiting small GTPases prenylation by using western blot analysis. We have found that Ftase II inhibitor dose-dependently inhibited prenylation of Rho A and Rho G in both 22Rv1 and C4-2B PCa cells. Also, exposure of Ftase I inhibitor to 22Rv1 cells only caused a marginal increase in Rho A prenylation but not Rho G. In fact, Ftases I treatment in C4-2B does not induce any changes in prenylation of Rho A and Rho G. In all these Ftases inhibitors treatment conditions, C4-2B cells treated with 10 and 20 μ M concentrations of ZOL was used as positive drug treatment control. These data also explain the fact that ZOL mediated inhibition of isoprenylation of Rho A and Rho G is because of inhibition of farnesylation of such small GTPases, which is similar to that of Ftases II (Supplementary Fig. S9A). Functionally, Ftases II inhibitor demonstrated significant reduction in number and growth of colonies of FDPS high/positive human and murine PTEN-deficient cells as compared to PTEN-sufficient cells (Supplementary Fig. S9B, C). Overall, our data provide mechanistic and functional insight into the association of FDPS and post-translational modification of small GTPases, in the promotion of PCa.

ZOL affects the colony formation, proliferation, and growth of PCa cells and 3D PCa tumoroids

ZOL treatment significantly decreased the number of colonies of human and murine PTEN-deficient PCa cells compared with respective untreated controls, as well as PTEN^{WT} 22Rv1 PCa cells ($P < 0.01$) (Fig. 6a, b). Cells treated with ZOL showed reduced growth from day 1 to day 7, compared to untreated cells (Supplementary Fig. S10A). Further, ZOL treatment decreased the proliferation of PCa cells at both 24 and 48 h (Supplementary Fig. S10B). Similarly, prostate tumoroids were treated with ZOL and assessed for growth inhibitory effects. Tumoroids treated with ZOL were more susceptible to growth inhibition compared to untreated controls ($P < 0.02$) (Fig. 6c, d). Viable cells were detected in control tumoroids and necrotic cells were observed in ZOL-treated tumoroids using hematoxylin and eosin staining (Fig. 6e). Our results suggest that ZOL could serve as a novel therapeutic

intervention for PCa. Based on the expression profile of FDPS in tumoroids (Fig. 1g), FDPS expression was analyzed in tumoroid sections treated with ZOL. A complete reduction of FDPS was observed in ZOL-treated tumoroids compared to untreated control tumoroids (Fig. 6e). These results suggest that inhibition of small GTPases protein prenylation via FDPS by ZOL will account for the reduced colony number, growth inhibition, and reduced proliferative capacity of PCa cells and 3D tumoroids. Thus, targeting FDPS might be an indirect mechanism to ameliorate PTEN-deficient PCa.

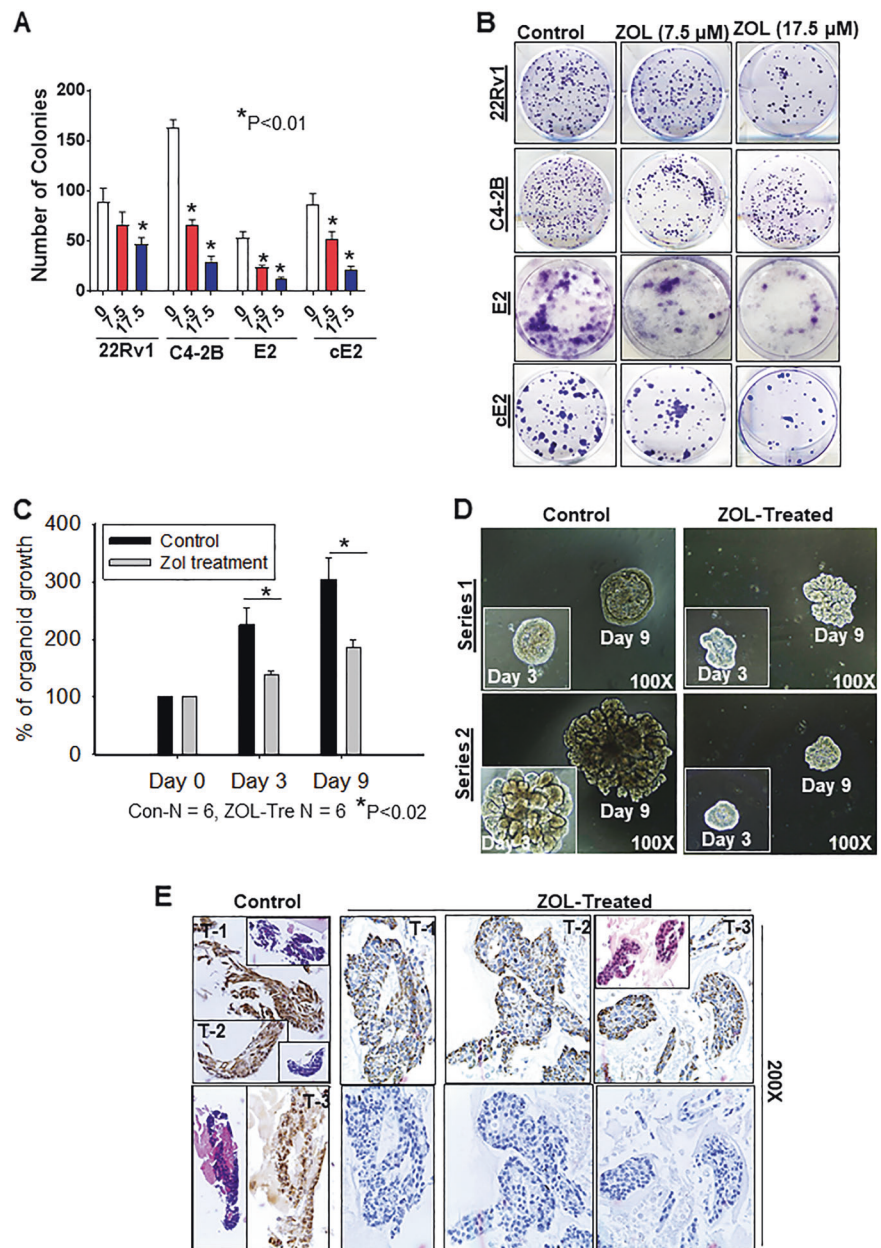
Discussion

The mevalonate pathway integrates all the metabolic pathways in cancer cells and plays a crucial role in cancer cell survival. FDPS is one of the molecules in the mevalonate pathway was shown to be upregulated in rat prostate [27] and human PCa tissues compared to benign prostate tissues [13]. The five major findings from this study are as follows: (a) loss of PTEN in mouse prostate resulted in aberrant expression of FDPS, but not with MYC-driven PCa; (b) FDPS was overexpressed in PTEN-inactive PCa cells, but not in PTEN-sufficient cells, which further supports a direct relationship between the PI3K pathway and FDPS; (c) FDPS expression in clinical PCa specimens indicates that FDPS is likely required for the initiation and progression of PTEN-deficient PCa tumors; (d) protein prenylation was identified as the key mechanism linking PTEN deficiency with FDPS elevation; and (e) targeting FDPS in PTEN deficient or PI3K activated status could reduce the number of colonies and inhibit proliferation of PCa cells through its effect on downstream AKT and ERK pathways. Collectively, our in vitro and in vivo evidence suggests that FDPS might be a novel target for PTEN-deficient PCa patients.

Previous studies demonstrate that elevated levels of FDPS correlate with PCa progression and tumor recurrence [13, 28], and a recent study also documents that FDPS mediated proliferation of glioblastoma cells [29]. Our observation of FDPS expression in PCa tissues is consistent with a recent global transcriptome analysis of PCa tissues demonstrating FDPS as one of five gene signatures specifically associated with PCa promotion [14]. We observed that FDPS was exclusively overexpressed in an autochthonous tumor from PTEN-deficient mice compared to Hi-Myc mice. Our results also demonstrated high FDPS expression at both protein and transcript levels in the majority of PTEN-deficient PCa cells, which correlated with AKT activation. Our analysis using publicly available databases showed FDPS was highly expressed in primary and metastatic PCa tissues, and that its gene frequency was altered in ~3–30% of PCa cases in which PTEN was either deleted or mutated at a frequency of

Fig. 6 Effects of ZOL in 2D and 3D tumoroid in vitro models.

a Colony formation assay was performed in human and mouse PCa cells. PTEN-deficient C4-2B, E2 and cE2 and PTEN-sufficient 22Rv1 cells were treated with and without ZOL ($N = 3/\text{treatment group}$) at indicated concentrations. After 14 days of incubation in complete medium, colonies were fixed with methanol, stained with crystal violet, and counted. Colony counts are expressed relative to untreated controls. Bar graphs represent data as mean \pm SE of triplicates. P values are denoted by asterisks ($P < 0.01$). **b** Representative images showing colonies formed by human and mouse PCa cells treated with and without ZOL. **c** The bar graph depicts average tumoroid growth with and without (control) ZOL treatment. **d** Light microscope images of representative tumoroids treated with and without ZOL on days 3, and 9. **e** H&E (Inset) and FDPS staining analysis on the tumoroids treated with and without ZOL along with negative controls (serial sections in bottom right panel)



~17.5–40% cases in the same cohort [30]. Recently, Chen and colleagues [31] showed that SREBP-dependent lipogenic signatures transform the minimally invasive PTEN-deficient prostate tumors into the metastatic disease. In an in vivo model of PCa, FDPS was shown to be dysregulated along with the SREBP family of proteins [28]. In line with these studies, FDPS was differentially expressed among murine PCa and normal prostate cells [8] and their derived organoids in our study.

How mevalonate pathway-associated genes are activated during oncogenesis and whether such activation affects its downstream targets and its biological consequences are largely unknown. In the current study, we observed that ectopic overexpression of FDPS significantly accelerated

growth and colony-forming ability of PTEN-deficient cells rather than PTEN-intact PCa cells by modulating the phosphorylation of AKT, ERK, and Cyclin B1, all critical for proliferation and survival of cancer cells. Of note, FDPS was shown to mediate the proliferative effect of sterols on hepatoblastoma cells [32], implying that FDPS alteration in the cancer cell may promote growth and proliferation. Loss of STAT1 has been associated with the pathobiology of several malignancies, including PCa [25], and we found that overexpression of FDPS reduced STAT1 phosphorylation at ser727 and Y701 in PCa cells. Based on the literature [15, 33, 34], we postulated that ectopic overexpression of FDPS could influence protein prenylation of small GTPases. Indeed, FDPS overexpression induced prenylation of small

GTPases such as Rho A, Rho G, CDC42, and H-Ras, which in turn is known to activate MAPK together with AKT signaling [35–38]. FDPS knockdown in glioblastoma cells affected the active forms of AKT, ERK, and STAT3 [29]. Consistent with these data, our FDPS knockdown studies showed inhibition of PCa cell growth via activation of AKT and ERK pathways. Of interest, forced overexpression of FDPS rescued the inhibitory effects of FDPS-targeting siRNAs. Thus, our data and previous studies raise the possibility of targeting FDPS to attenuate activation of ERK, AKT, and STAT1 signaling in aggressive PCa.

Previously, a study demonstrated that upregulation of mevalonate pathway genes along with activation of the PI3K/AKT pathway supported growth in colon cancer stem cells [39]. Hence, we verified that direct inhibition of PI3K, but not AKT phosphorylation, is sufficient to reduce FDPS expression. ZOL, a nitrogen-containing bisphosphate, was previously used to treat bone resorption in prostate and breast cancer cells and known to aid in reducing and delaying bone complications [40, 41]. ZOL was later shown to function as an anti-tumor agent by inhibiting proliferation and promoting apoptosis [20]. Recent studies show that ZOL could inhibit FDPS by directly binding to active enzyme sites [12, 18, 42]. Building on those studies, we observed ZOL inhibited growth and colony formation to a greater extent in PTEN-deficient PCa cells than in PTEN-sufficient cells through inhibition of phosphorylation of AKT and ERK in human and mouse PCa cells. The recent development of syngenic cell lines and 3D organoids/tumoroids from genetically modified mice has made preclinical studies easier to develop [43]. Our data on mPCa tumoroids showed decreased growth rate following 24 h exposure to ZOL. These observations are in agreement with the *in vitro* efficacy of ZOL in renal cell carcinoma cells [44]. Overall, these molecular and functional actions of ZOL may predict its synergy if combined with chemo or radiation treatment.

Our study demonstrated both the clinical and translational relevance of FDPS in PCa. Primarily, the increased expression of FDPS along the continuum from non-neoplastic to prostate tissue suggests prolonged activation of AKT/ERK and suppression of STAT1 may be facilitating the inflammatory process underlying disease progression. In the future, this work could be extended to investigate the role of FDPS in PCa metastasis, as well as its correlation with PSA level and survival in PCa patients. Second, our data suggest a mechanism by which PTEN-deficient cells mediates cancer cell survival by its ability to activate metabolic oncogene FDPS. In fact, these metabolic changes within a tumor may also contribute to therapy resistance by increasing intratumoral androgens [4, 45]. Finally, this is the first work supporting re-purposing of ZOL to target FDPS in PTEN-deficient PCa, which would be a novel approach to enhance PCa combination therapies in the future (Fig. 7).

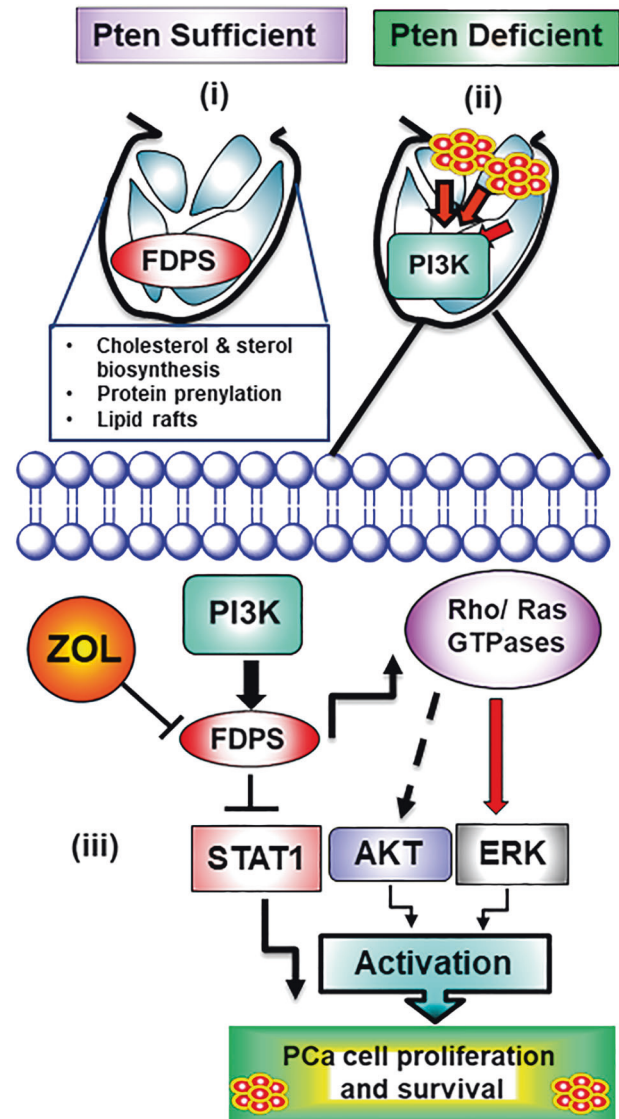


Fig. 7 Schematic diagram showing the critical role of FDPS in normal prostate and prostate cancer and its associated potential mechanism(s). (i) FDPS is a crucial intermediate enzyme required for cholesterol and sterol biosynthesis. This enzyme catalyzes production of geranyl pyrophosphate and farnesyl pyrophosphate from isopentenyl pyrophosphate and dimethyl-allyl pyrophosphate. Apart from enzyme catalysis, FDPS is involved in post-translational modifications (protein prenylation) of GTPases. Inactivation of FDPS through interferon disrupts specialized cell membrane-associated microdomains, such as lipid rafts, required for protein and receptor trafficking, cell signaling, and neurotransmission regulation. (ii) FDPS is overexpressed in prostate cancer and associated with tumor recurrence. FDPS also regulates intratumoral androgens, which further interferes with ADT therapy in the localized and locally advanced stages of prostate cancer. (iii) Flow diagram describes various mechanisms associated with FDPS overexpression in prostate cancer cells. FDPS may be stimulated by androgens and ectopic overexpression of FDPS resulted in activation of AKT and ERK signaling for sustained proliferative signals, but deactivates STAT1 pathway, disrupting its tumor suppressive function. ZOL potentially inhibits FDPS thereby modulating the prenylation of small GTPases resulting in deactivation of AKT, ERK, and STAT signaling in prostate cancer cells

Materials and methods

Tissue microarray and immunohistochemistry

Specimen details, clinical information, and pathological scoring are given in the Supplementary materials and methods. Immunohistochemistry procedures were adapted from our previous report [46].

Generation of mouse models of PCa and their derived tumoroids

PTEN conditional knockout (cKO), Hi-Myc, and littermate wild-type mice generation, characterization and their derived organoids and syngenic cell lines are described in Supplementary materials and methods. Primers used for PCR genotyping are listed in Supplementary Table S5. The tumoroids generation procedure was adapted from previous publications [47].

Cell culture and reagents

All PCa cell lines were cultured and maintained as previously described [48]. See Supplementary materials and methods for details about human and mouse PCa cell lines [49], their genomic identity details, and treatments with ZOL, DHT, PI3K inhibitor (PI-103), AKT inhibitor (MK-2206), Simvastatin, Fluvastatin, Farnesyl transferase inhibitors I, and Farnesyl transferase inhibitors II drugs.

RNA isolation and quantitative real-time PCR analysis

RNA isolation and real-time PCR were performed as described in our previous publication [50].

Primer details are described in Supplementary Table S5.

Western blot analysis

Descriptions of ZOL treatment in PCa cells, cells harvesting, and routine western blot analysis are given in Supplementary materials and methods. Primary antibodies with respective dilutions are listed in Supplementary Table. S6.

Databases analysis

Detailed methods adapted for database analysis are given in Supplementary materials and methods.

Overexpression and siRNA constructs and transfection

For overexpression construct design (FDPS) and siRNA transient (FDPS, PI3K, AKT, P53) and stable transfection procedures, see Supplementary materials and methods.

Confocal microscopy

Confocal analysis was performed as described in our earlier publication [50] and summarized in Supplementary materials and methods.

Colony formation assay

Colony formation assay was performed as described in our previous publication [46].

MTT cytotoxicity assay for IC₂₅ determination

MTT assay was performed as per the standard procedure [12].

Growth kinetics and proliferation assays

Growth kinetics assay was performed in 22Rv1, C4-2B, and cE2 human and mouse PCa cells as per our previous publication [50]. For additional details, see Supplementary materials and methods.

Statistical analysis

Statistical analysis of the groups were briefly described in Supplementary materials and methods.

Acknowledgements We thank Jessica Mercer for her editorial contribution to the paper. We also greatly appreciate the technical help of Ms. Garima Kaushik, Ms. Pranita Atri, and Ms. Kavita Mallya.

Funding This work/authors are supported, in parts, by the grants from the United States Department of Defense Grant PC170891, National Institutes of Health (P01 CA217798, U01 CA185148 and 1R01CA182435-01A1) and P30 GM106397.

Compliance with ethical standards

Conflict of interest SKB is one of co-founders of Sanguine Diagnostics and Therapeutics, Inc. The remaining authors declare that they have no conflicts of interest.

Publisher's note: Springer Nature remains neutral with regard to jurisdictional claims in published maps and institutional affiliations.

References

- Siegel RL, Miller KD, Jemal A. Cancer statistics, 2019. *CA Cancer J Clin*. 2019;69:7–34.
- Bastian PJ, Boorjian SA, Bossi A, Briganti A, Heidenreich A, Freedland SJ, et al. High-risk prostate cancer: from definition to contemporary management. *Eur Urol*. 2012;61:1096–106.
- Taylor LG, Canfield SE, Du XL. Review of major adverse effects of androgen-deprivation therapy in men with prostate cancer. *Cancer*. 2009;115:2388–99.
- Leon CG, Locke JA, Adomat HH, Etinger SL, Twiddy AL, Neumann RD, et al. Alterations in cholesterol regulation contribute to the production of intratumoral androgens during progression to castration-resistant prostate cancer in a mouse xenograft model. *Prostate*. 2010;70:390–400.
- Yue S, Li J, Lee SY, Lee HJ, Shao T, Song B, et al. Cholesteryl ester accumulation induced by PTEN loss and PI3K/AKT activation underlies human prostate cancer aggressiveness. *Cell Metab*. 2014;19:393–406.
- Allott EH, Howard LE, Cooperberg MR, Kane CJ, Aronson WJ, Terris MK, et al. Serum lipid profile and risk of prostate cancer recurrence: results from the SEARCH database. *Cancer Epidemiol Biomark Prev*. 2014;23:2349–56.
- Ferraldeschi R, Nava Rodrigues D, Riisnaes R, Miranda S, Figueiredo I, Rescigno P, et al. PTEN protein loss and clinical outcome from castration-resistant prostate cancer treated with abiraterone acetate. *Eur Urol*. 2015;67:795–802.
- Wang S, Gao J, Lei Q, Rozengurt N, Pritchard C, Jiao J, et al. Prostate-specific deletion of the murine Pten tumor suppressor gene leads to metastatic prostate cancer. *Cancer Cell*. 2003;4:209–21.
- Taylor BS, Schultz N, Hieronymus H, Gopalan A, Xiao Y, Carver BS, et al. Integrative genomic profiling of human prostate cancer. *Cancer Cell*. 2010;18:11–22.
- Grasso CS, Wu YM, Robinson DR, Cao X, Dhanasekaran SM, Khan AP, et al. The mutational landscape of lethal castration-resistant prostate cancer. *Nature*. 2012;487:239–43.
- Fraser M, Sabelnykova VY, Yamaguchi TN, Heisler LE, Livingstone J, Huang V, et al. Genomic hallmarks of localized, non-indolent prostate cancer. *Nature*. 2017;541:359–64.
- Soucek JJ, Baine MJ, Lin C, Rachagani S, Gupta S, Kaur S, et al. Unbiased analysis of pancreatic cancer radiation resistance reveals cholesterol biosynthesis as a novel target for radiosensitisation. *Br J Cancer*. 2014;111:1139–49.
- Todenhof T, Hennenlotter J, Kuhs U, Gerber V, Gakis G, Vogel U, et al. Altered expression of farnesyl pyrophosphate synthase in prostate cancer: evidence for a role of the mevalonate pathway in disease progression? *World J Urol*. 2013;31:345–50.
- Long Q, Xu J, Osunkoya AO, Sannigrahi S, Johnson BA, Zhou W, et al. Global transcriptome analysis of formalin-fixed prostate cancer specimens identifies biomarkers of disease recurrence. *Cancer Res*. 2014;74:3228–37.
- Bifulco M. Role of the isoprenoid pathway in ras transforming activity, cytoskeleton organization, cell proliferation and apoptosis. *Life Sci*. 2005;77:1740–9.
- Reilly JE, Neighbors JD, Hohl RJ. Targeting protein geranylgeranylation slows tumor development in a murine model of prostate cancer metastasis. *Cancer Biol Ther*. 2017;18:872–82.
- Algur E, Macklis RM, Hafeli UO. Synergistic cytotoxic effects of zoledronic acid and radiation in human prostate cancer and myeloma cell lines. *Int J Radiat Oncol Biol Phys*. 2005;61:535–42.
- Gritzalis D, Park J, Chiu W, Cho H, Lin YS, De Schutter JW, et al. Probing the molecular and structural elements of ligands binding to the active site versus an allosteric pocket of the human farnesyl pyrophosphate synthase. *Bioorg Med Chem Lett*. 2015;25:1117–23.
- Jagdev SP, Coleman RE, Shipman CM, Rostami HA, Croucher PI. The bisphosphonate, zoledronic acid, induces apoptosis of breast cancer cells: evidence for synergy with paclitaxel. *Br J Cancer*. 2001;84:1126–34.
- Ottewell PD, Monkkonen H, Jones M, Lefley DV, Coleman RE, Holen I. Antitumor effects of doxorubicin followed by zoledronic acid in a mouse model of breast cancer. *J Natl Cancer Inst*. 2008;100:1167–78.
- Ozturk OH, Bozcuk H, Burgucu D, Ekin D, Ozdogan M, Akca S, et al. Cisplatin cytotoxicity is enhanced with zoledronic acid in A549 lung cancer cell line: preliminary results of an in vitro study. *Cell Biol Int*. 2007;31:1069–71.
- Ullen A, Lennartsson L, Harmenberg U, Hjelm-Eriksson M, Kalkner KM, Lennernas B, et al. Additive/synergistic antitumoral effects on prostate cancer cells in vitro following treatment with a combination of docetaxel and zoledronic acid. *Acta Oncol*. 2005;44:644–50.
- Kwak MK, Johnson DT, Zhu C, Lee SH, Ye DW, Luong R, et al. Conditional deletion of the Pten gene in the mouse prostate induces prostatic intraepithelial neoplasms at early ages but a slow progression to prostate tumors. *PLoS ONE*. 2013;8:e53476.
- Ellwood-Yen K, Graeber TG, Wongvipat J, Iruela-Arispe ML, Zhang J, Matusik R, et al. Myc-driven murine prostate cancer shares molecular features with human prostate tumors. *Cancer Cell*. 2003;4:223–38.
- Hatzieremia S, Mohammed Z, McCall P, Willder JM, Rosewicz AK, Underwood MA, et al. Loss of signal transducer and activator of transcription 1 is associated with prostate cancer recurrence. *Mol Carcinog*. 2016;55:1667–77.
- Li L, Chen GP, Yang Y, Ye Y, Yao L, Hu SJ. Chronic inhibition of farnesyl pyrophosphate synthase attenuates cardiac hypertrophy and fibrosis in spontaneously hypertensive rats. *Biochem Pharmacol*. 2010;79:399–406.
- Heemers H, Maes B, Fougelle F, Heyns W, Verhoeven G, Swinnen JV. Androgens stimulate lipogenic gene expression in prostate cancer cells by activation of the sterol regulatory element-binding protein cleavage activating protein/sterol regulatory element-binding protein pathway. *Mol Endocrinol*. 2001;15:1817–28.
- Etinger SL, Sobel R, Whitmore TG, Akbari M, Bradley DR, Gleave ME, et al. Dysregulation of sterol response element-binding proteins and downstream effectors in prostate cancer during progression to androgen independence. *Cancer Res*. 2004;64:2212–21.
- Abate M, Laezza C, Pisanti S, Torelli G, Seneca V, Catapano G, et al. Deregulated expression and activity of farnesyl diphosphate synthase (FDPS) in glioblastoma. *Sci Rep*. 2017;7:14123.
- Cerami E, Gao J, Dogrusoz U, Gross BE, Sumer SO, Aksoy BA, et al. The cBio cancer genomics portal: an open platform for exploring multidimensional cancer genomics data. *Cancer Discov*. 2012;2:401–4.
- Chen M, Zhang J, Sampieri K, Clohessy JG, Mendez L, Gonzalez-Billalabeitia E, et al. An aberrant SREBP-dependent lipogenic program promotes metastatic prostate cancer. *Nat Genet*. 2018;50:206–18.
- Ishimoto K, Tachibana K, Hanano I, Yamasaki D, Nakamura H, Kawai M, et al. Sterol-regulatory-element-binding protein 2 and nuclear factor Y control human farnesyl diphosphate synthase expression and affect cell proliferation in hepatoblastoma cells. *Biochem J*. 2010;429:347–57.
- Dhar MK, Koul A, Kaul S. Farnesyl pyrophosphate synthase: a key enzyme in isoprenoid biosynthetic pathway and potential molecular target for drug development. *N Biotechnol*. 2013;30:114–23.
- Cox AD, Der CJ. The ras/cholesterol connection: implications for ras oncogenicity. *Crit Rev Oncog*. 1992;3:365–400.

35. Wang J, Yuan Y, Zhou Y, Guo L, Zhang L, Kuai X, et al. Protein interaction data set highlighted with human Ras-MAPK/PI3K signaling pathways. *J Proteome Res.* 2008;7:3879–89.
36. Castellano E, Downward J. RAS Interaction with PI3K: more than just another effector pathway. *Genes Cancer.* 2011;2:261–74.
37. Beier F, Loeser RF. Biology and pathology of Rho GTPase, PI-3 kinase-Akt, and MAP kinase signaling pathways in chondrocytes. *J Cell Biochem.* 2010;110:573–80.
38. Maltese WA. Posttranslational modification of proteins by isoprenoids in mammalian cells. *FASEB J.* 1990;4:3319–28.
39. Sharon C, Baranwal S, Patel NJ, Rodriguez-Agudo D, Pandak WM, Majumdar AP, et al. Inhibition of insulin-like growth factor receptor/AKT/mammalian target of rapamycin axis targets colorectal cancer stem cells by attenuating mevalonate-isoprenoid pathway in vitro and in vivo. *Oncotarget.* 2015;6:15332–47.
40. Karabulut B, Erten C, Gul MK, Cengiz E, Karaca B, Kucukzeybek Y, et al. Docetaxel/zoledronic acid combination triggers apoptosis synergistically through downregulating anti-apoptotic Bcl-2 protein level in hormone-refractory prostate cancer cells. *Cell Biol Int.* 2009;33:239–46.
41. Neville-Webbe HL, Coleman RE, Holen I. Combined effects of the bisphosphonate, zoledronic acid and the aromatase inhibitor letrozole on breast cancer cells in vitro: evidence of synergistic interaction. *Br J Cancer.* 2010;102:1010–7.
42. Dunford JE, Thompson K, Coxon FP, Luckman SP, Hahn FM, Poulter CD, et al. Structure-activity relationships for inhibition of farnesyl diphosphate synthase in vitro and inhibition of bone resorption in vivo by nitrogen-containing bisphosphonates. *J Pharmacol Exp Ther.* 2001;296:235–42.
43. Gao D, Vela I, Sboner A, Iaquinta PJ, Karthaus WR, Gopalan A, et al. Organoid cultures derived from patients with advanced prostate cancer. *Cell.* 2014;159:176–87.
44. Kijima T, Koga F, Fujii Y, Yoshida S, Tatokoro M, Kihara K. Zoledronic acid sensitizes renal cell carcinoma cells to radiation by downregulating STAT1. *PLoS ONE.* 2013;8:e64615.
45. Hirschey MD, DeBerardinis RJ, Diehl AM, Drew JE, Frezza C, Green MF, et al. Dysregulated metabolism contributes to oncogenesis. *Semin Cancer Biol.* 2015;35:Suppl: S129–150.
46. Hein AL, Seshacharyulu P, Rachagani S, Sheinin YM, Ouellette MM, Ponnusamy MP, et al. PR55alpha subunit of protein phosphatase 2A supports the tumorigenic and metastatic potential of pancreatic cancer cells by sustaining hyperactive oncogenic signaling. *Cancer Res.* 2016;76:2243–53.
47. Kaushik G, Ponnusamy MP, Batra SK. Current status of 3-D organoids as pre-clinical models. *Stem Cells.* 2018;36:1329–40.
48. Muniyan S, Chen SJ, Lin FF, Wang Z, Mehta PP, Batra SK, et al. ErbB-2 signaling plays a critical role in regulating androgen-sensitive and castration-resistant androgen receptor-positive prostate cancer cells. *Cell Signal.* 2015;27:2261–71.
49. Liao CP, Liang M, Cohen MB, Flesken-Nikitin A, Jeong JH, Nikitin AY, et al. Mouse prostate cancer cell lines established from primary and postcastration recurrent tumors. *Horm Cancer.* 2010;1:44–54.
50. Lakshmanan I, Rachagani S, Hauke R, Krishn SR, Paknikar S, Seshacharyulu P, et al. MUC5AC interactions with integrin beta4 enhances the migration of lung cancer cells through FAK signaling. *Oncogene.* 2016;35:4112–21.